Current Collection by a Long Conducting Cylinder in a Flowing Magnetized Plasma

Bharat I. Vashi* and Nagendra Singh†
University of Alabama in Huntsville, Huntsville, Alabama 35899

The current collection by a conducting cylinder in a plasma through the transport of charged particles across a magnetic field is studied by means of numerical simulations. An electrostatic particle-in-cell code is used. The conducting cylinder is oriented along an ambient magnetic field B_0. The plasma flows with an unperturbed relative velocity V_0 perpendicular to B_0. The potential structure near a positively biased cylinder is investigated. The potential structure is found to be dynamic and azimuthally asymmetric. The electric fields in the structure create a two-cell circulation of the electrons near the cylinder. The cell in the wake region has negative potentials. A fan-shaped circulation cell forms around the cylinder, and in this cell, the potential is generally positive. The geometry and the size of this positive cell affects the current collection. The time-averaged current is found to vary approximately linearly with the flow velocity V_0. For the typical value of V_0 ($\sim$ 8 km/s) in the low Earth orbit, the enhancement in the current through the cross-field plasma transport is found to be an appreciable fraction of the current predicted by the existing models, which do not account for the cross-field plasma transport. The cross-field transport is affected primarily by the asymmetrical sheath structure.

Nomenclature

$\hat{a}_y$ = unit vector along y axis of the Cartesian coordinate
$\boldsymbol{B_0}$ = ambient magnetic field
$\boldsymbol{E}$ = electric field
$\boldsymbol{E_0}$ = convection field
$\boldsymbol{E_1}$ = electric field associated with space charges
e = magnitude of electronic charge
I = current collected by the cylinder
k_B = Boltzmann constant
$m_{c\alpha}$ = mass of computer particles
m_e = electron mass
m_i = ion mass
$m_{r\alpha}$ = mass of real particle
$N_{c\alpha}$ = density of computer particle
N_{inj} = number of charged particles injected at each time step
$N_{r\alpha}$ = density of real particle
N_0 = ambient plasma density
q_α = charge on a computer particle
$R_{\max}$ = radial size of the simulation system
r = radial distance
$\tilde{r}$ = r/λ_{d0}
r_s = radius of conducting cylinder
$T_{c\alpha}$ = temperature of computer particle
T_e = electron temperature
$T_{r\alpha}$ = temperature of real particle
T_0 = ambient electron temperature
t = time
$\tilde{t}$ = $t\omega_{p0}$
$\tilde{V}_0$ = V/V_{te}
V_{te} = $(k_BT_e/m_e)^{1/2}$
V_0 = flow velocity
α = charge particle species, = e or i
Δr = radial grid spacing
Δt = time step for advancing the simulation
$\Delta\theta$ = angular grid spacing
δN_α = number of computer particles collected during a time step
ϵ_0 = permittivity of free space
θ = angular coordinate
λ_{d0} = plasma Debye length
ρ = charge density
ρ_e = electron Larmor radius
ϕ = potential
$\tilde{\phi}$ = ϕ/ϕ_n
ϕ_n = kT_e/e
ϕ_0 = bias potential
ω_{p0} = electron plasma frequency in the ambient plasma

I. Introduction

THERE is renewed interest in the current-collection properties of bodies in space plasmas. The motivation for this arises from several applications, such as the tethered-satellite systems, charge neutralization on space vehicles, and active experiments involving injections of charged-particle beams from space vehicles. The problem of current collection involves interaction of the space plasma with a moving collecting body biased at some potential with respect to the ambient plasma. In the low Earth orbit, the electrons are highly magnetized as their Larmor radius $\rho_e \simeq 3$ cm while the size of the current collector $d > 1$ m. Since, in such a situation, electrons are effectively guided by the magnetic field, Parker and Murphy[1] have shown that the current collection is highly limited and the major contribution to the current comes from the motion of electrons parallel to the magnetic field. Linson[2] has argued that the plasma turbulence in the vicinity of a body at a relatively high potential causes diffusion of electrons across the magnetic field lines and, therefore, a relatively much larger current than that predicted by the Parker-Murphy model can be collected. However, this suggestion of Linson[2] concerning the effects of cross-field transport of electrons on the current

Presented as Paper 90-0724 at the AIAA 28th Aerospace Sciences Meeting, Reno, NV, Jan. 8-11, 1990; received Jan. 29, 1990; first revision received Sept. 21, 1990; second revision received Dec. 3, 1990; accepted for publication Dec. 4, 1990.

*Graduate Student, Department of Electrical Engineering, Center for Space Plasma and Aeronomic Research.

†Professor, Department of Electrical Engineering, Center for Space Plasma and Aeronomic Research. Member AIAA.

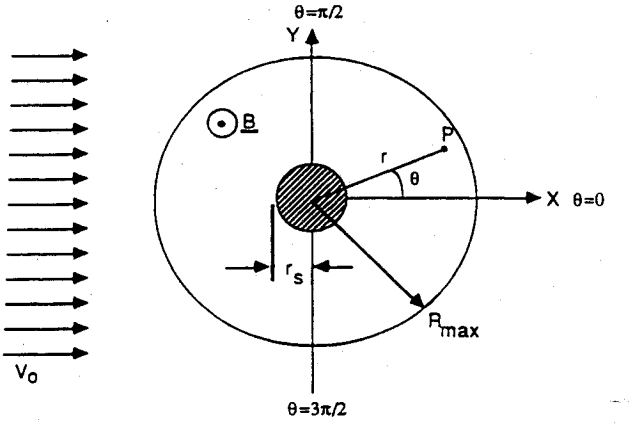

Fig. 1 Geometry of the simulation. The conducting cylinder is shown by the hatched region. The magnetic field is parallel to the axis of the cylinder.

collection has never been checked rigorously. The main goal of this paper is to examine this issue by means of numerical simulations of plasma flow past a long conducting cylinder with the magnetic field along the axis of the cylinder (Fig. 1). We have purposely chosen these geometrical features to highlight the effect of cross-field plasma transport on the current collection without any contribution to the current from the field-aligned motion of the plasma particles.

Our simulations show that the cross-field transport of electrons does enhance the electron collection, but the plasma turbulence is not seen to play the key role in the transport process. It is the modified potential structure around the cylinder and the associated circulation of the electrons around the cylinder that are found to effectively control the current collection. The interaction of the flowing plasma with the positive cylinder sets up a two-cell circulation pattern. The circulation pattern in the wake is determined by the electric fields in a negative potential well. Another circulation pattern develops around the cylinder and it may encompass a relatively large area in front of the cylinder. In this cell, the potential is generally positive. Thus, the effect of the positive potential on the cylinder may extend to a relatively large distance from it. This leads to an enhancement in the collection of electrons by the cylinder. For relatively large flow velocities, the two cells coexist in a quasisteady state, but for relatively low flow velocities, the two cells are seen to mutually interact, affecting each other. When the negative cell dominates, the collected current is low. When the positive cell dominates, the collected current is appreciably enhanced. This leads to a relaxation type of oscillation in the collected current. The time-averaged current is found to vary approximately linearly with the flow velocity. For the typical orbital velocity of 8 km/s in the ionosphere, the enhancement in the current collection through the cross-field transport is found to be an appreciable fraction of the current predicted by the Parker-Murphy model.[1] Recently, Myers et al.[3] reported that the current collection by a rocket body in the ionosphere agrees remarkably well with the Parker-Murphy model. We attribute this to the low velocity of the rocket body; the typical value of the component of the rocket velocity perpendicular to the ambient magnetic field is generally < 100 m/s, for which the enhancement in the current due to the cross-field plasma transport is found to be negligibly small.

The rest of the paper is organized as follows. The numerical technique, the definitions, and the normalizations used in the simulations are described in Sec. II. Numerical results are presented in Sec. III. In this section we have examined the potential structure around the cylinder, its effect on the current collection, and its oscillatory behavior. The variation of the time-averaged current as a function of the relative motion between the plasma and the cylinder is examined here. The paper is concluded in Sec. IV.

II. Simulation Technique

System Solution

The plasma flow past the cylinder is simulated, as shown in Fig. 1. The hatched area is the end view of the long conducting cylinder of radius r_s. In the rest frame of the cylinder, plasma flows along the positive X direction with the velocity V_0. The flow is facilitated by imposing a dc convection electric field along the Y axis given by $E_0 = V_0 B$. The simulated plasma region is limited to $r \le R_{max}$ (Fig. 1). At the initial time $t = 0$, the simulation region is a vacuum and the plasma flow for $t > 0$ is maintained by injecting charged particles at the rim of the simulation box ($r = R_{max}$) over the angular region $\pi/2 \le \theta \le 3\pi/2$ (Fig. 1). The average injection velocity of the charged particles is V_0. At each time step, a predetermined number (N_{inj}) of electron-ion pairs are injected to simulate a desired plasma flux. The plasma particles used in the simulations are like rods parallel to the magnetic field.[4] Except for some details, the simulation technique used here is similar to that used by Thiemann et al.[5] The injected particles are chosen from Maxwellian distributions with equal electron and ion temperatures T_0. The Y coordinates of the particles are chosen according to a uniform probability distribution. The X coordinates are first calculated by $X = (R_{max}^2 - y^2)^{1/2}$ and then further randomized by replacing X by $X + V\Delta t$ where V is the particle velocity randomly chosen from a Maxwellian distribution and Δt is the time step. Our injection technique is quite similar to that described by Aldrich.[6]

The magnitude of charge q_α, per unit length of such computer particles, is obtained by balancing the plasma flux into the simulation region at the injection boundary and the simulated flux due to the injection of the charge particles at each time step of duration Δt, giving

$$|q_\alpha| = 2R_{max} e N_0 V_0 \Delta t / N_{inj} \text{ C/m} \tag{1}$$

The injection of equal numbers of electrons and ions insures that no net charge is injected into the system.

The temporal and spatial evolutions of the plasma and fields are calculated by the self-consistent solutions of the equations of motions of all of the charged particles and the Poisson equation for the electric potential ϕ. It is important to note that, in our simulations, the electric field has two contributions, as indicated by the following equation:

$$E = E_0 \hat{a}_y + E_1 \tag{2}$$

Since E_0 is uniform in space, $\nabla \cdot E_0 = 0$ and the divergence of Eq. (2) gives

$$\nabla \cdot E = \nabla \cdot E_1 = \rho/\epsilon_0 \tag{3}$$

Under the electrostatic approximation, $E_1 = -\nabla\phi$ and Eq. (3) gives the Poisson equation

$$\nabla^2 \phi = -\rho/\epsilon_0 \tag{4}$$

The boundary conditions on the electric potential ϕ are $\phi(r = r_s, \theta) = \phi_0$ and $\phi(r = R_{max}, \theta) = 0$. The particles striking the cylinder and those leaving the system are assumed to be lost. However, the simulation system is maintained quasineutral at the global scale. For this purpose, we compare the total numbers of electrons and ions in the entire system at each time step. The deficit charged particles, which are taken from a Maxwellian plasma reservoir, are randomly distributed over the entire simulation system according to a uniform probability distribution. If such a global quasineutrality is not maintained, the system becomes quite noisy due to fast spurious oscillations. It is important to point out that the global quasineutrality does not imply local charge neutrality inside the sheath structure.

The collected current I is calculated by counting the electrons and ions striking the cylinder during each time step,

$$I = \sum_{\alpha} q_\alpha \delta N_\alpha / \Delta t \tag{5}$$

where q_α is given by Eq. (1). We note that, although q_α depends on the numerical factors $R_{\max}$, N_{inj}, and Δt, the current I is found to be independent of them if $R_{\max}$ and N_{inj} are sufficiently large and Δt is sufficiently small.

Normalizations and Definitions

We discussed earlier that the charge on a computer particle is given by Eq. (1). If $q_\alpha/e = \eta$, the analogy between the real and computer particles requires that the masses m, effective temperatures T, and density N satisfy the relations

$$m_{c\alpha} = \eta m_{r\alpha}, \qquad T_{c\alpha} = \eta T_{r\alpha}, \qquad N_{c\alpha} = N_{r\alpha}/\eta \tag{6}$$

where the subscripts r and c refer to the real and computer particles, respectively. It is worth mentioning that the electron and ion Debye lengths and plasma frequencies are invariant under the scaling law described by Eq. (6).

The results presented in this paper are based on simulations with the following ionospheric plasma parameters: ambient plasma density $N_0 = 10^{11}$ m^{-3}, electron temperature $T_e = 0.2$ eV, plasma Debye length $\lambda_{d0} \simeq 1$ cm, electron plasma frequency $\omega_{p0} \simeq 1.8 \times 10^7$ rad/s, and the magnetic field $\boldsymbol{B}_0 = 0.3$ G.

To simplify the equations and to generalize the applicability of their solutions to different situations with varying plasma and current-collector parameters, we use the following normalizations: potential $\tilde{\phi} = \phi/\phi_n$, $\phi_n = k_B T_e/e$; time $\tilde{t} = t\omega_{p0}$; velocity $\tilde{V} = V_{te}$, $V_{te} = (k_B T_e/m_e)$, and distance $\tilde{r} = r/\lambda_{d0}$.

In view of these normalizations, the Poisson equation (4) can be written as

$$\frac{\partial^2\tilde{\phi}}{\partial\tilde{r}^2} + \frac{1}{\tilde{r}}\frac{\partial^2\tilde{\phi}}{\partial\tilde{r}} + \frac{1}{\tilde{r}^2}\frac{\partial^2\tilde{\phi}}{\partial\theta^2} = -\frac{\lambda_{d0}^2}{\phi_n}(qn_{\text{ic}} - qn_{\text{ec}}) \tag{7}$$

where qn_{ic} and qn_{ec} are the charge per unit volume associated with the computer ions and electrons, respectively. It is assumed that both types of particles have the same magnitude of charge, i.e., $q_e = q_i = q$, as given by Eq. (1). These charge densities (qn_{ic} and qn_{ec}) are determined by calculating the number of computer particles at each grid point by the area sharing method[4] and dividing it by the effective volume of a cell. This volume is given by $r_j \Delta\theta \Delta r \Delta z$, where r_j is the radial distance of a grid point, and Δz is the length along the axial direction. With these definitions and Eq. (1), the normalized Poisson equation takes the form

$$\frac{\partial^2\tilde{\phi}}{\partial\tilde{r}^2} + \frac{1}{\tilde{r}}\frac{\partial\tilde{\phi}}{\partial\tilde{r}} + \frac{1}{\tilde{r}^2}\frac{\partial\tilde{\phi}}{\partial\theta^2} = -2\tilde{R}_{\max}\tilde{V}_0\Delta\tilde{t}(\Delta n_{\text{ic}} - \Delta n_{\text{ec}})/\tilde{r}_j\Delta\tilde{r}\Delta\theta N_{\text{inj}} \tag{8}$$

where Δn_{ic} and Δn_{ec} are the number of computer ions and electrons shared on a grid point ($j\Delta r$, $i\Delta\theta$). Equation (8) is differenced and solved by the Gaussian-elimination method.

The numerical results presented in the following are based on the following numerical parameters: $R_{\max} = 140\lambda_{d0} \approx 1.4$ m, $r_s = 10\lambda_{d0} \approx 0.1$ m, $\Delta\tilde{t} = 0.2$, $\Delta\tilde{r} = 1$, $\Delta\theta = 10$ deg, and the normalized flow velocity $\tilde{V}_0 = V_0/V_{te}$ is varied. For the purpose of computational economy, we have used an artificial ion to electron mass ratio $m_i/m_e = 100$. We note that in our simulation electron cyclotron period $\tau_{ce} \approx 18\,\omega_{p0}^{-1}$, whereas the ion cyclotron period $\tau_{ci} \simeq 1800\,\omega_{p0}^{-1}$. Thus, for the time scales in the simulations, electrons are magnetized and ions behave as unmagnetized charged particles.

III. Numerical Results

We begin the simulations with no plasma in the system. In response to the injection of charged particles starting at $t = 0$, plasma builds up in the system, as shown in Figs. 2a and 2b, which show the temporal evolutions of the distributions of electrons and ions, respectively. Each dot in these figures represents a computer particle. The plots at $\tilde{t} = 300$ show that the simulation system is already filled with a large number of electrons and ions. The plot for the ions shows the extended void region with no ions in it. This is the signature of the wake behind the cylinder. Even the electrons show a void region in a direction of about 45 deg from the ram direction, as indicated by an x in the panel for the $\tilde{t} = 300$. The difference between the electron and ion voids is due to the fact that, at the time scale of interest here, the $\boldsymbol{E}_1 \times \boldsymbol{B}_0$ drift affects the electrons whereas the unmagnetized ions are not affected by it. We note the presence of a crescent of a dense plasma in front of the cylinder. This gives an appearance of a bow shock.

The plots for $\tilde{t} > 300$ show that the ion wake behind the cylinder fills with increasing time, but in the rest of the region, the configuration of the plasma reaches a quasisteady state after about $\tilde{t} \gtrsim 400$. The main features of this state are as follows. We note a ring of void near the cylinder from which ions are totally absent. This is expected because the cylinder is positively biased. The crescent of the dense plasma persists in front of the cylinder, although it undergoes some variation with time as a result of plasma processes described later. A careful examination of the electron distribution shows that an extended low density region exists near the cylinder (indicated by x) and it undergoes an oscillatory rotation. The cause of this rotation and its association with the potential structure near the cylinder is described in the following discussion.

We now present results from the simulations showing cross-field plasma transport and its effect on current collection by the cylinder. Figure 3 shows the temporal evolution of the current for three drift velocities ($\tilde{V}_0 = 0.3$, 0.5, and 0.8) and for the bias potential $\tilde{\phi}_0 = 50$. The currents shown here are averaged over fast oscillations. As evident from the figure, the computer runs for each drift were carried out for different lengths of the normalized time $\tilde{t}$. The curves in Fig. 3 show that there is a transient phase in which currents build up from zero to steady-state average values, as shown by the dotted horizontal lines for each value of V_0. However, the currents are seen to oscillate about the average values. The average values of the currents are found to vary approximately linearly

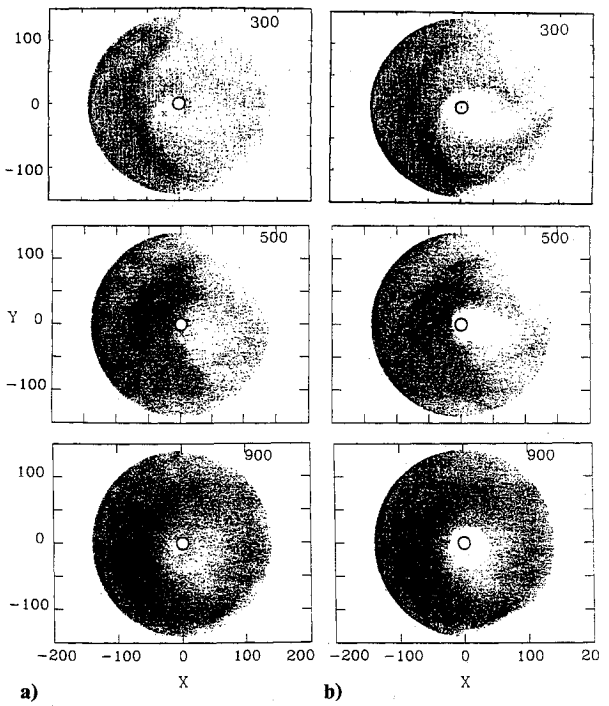

Fig. 2 Temporal evolutions of the distributions of a) electrons and b) ions around the cylinder shown by the ring in the center.

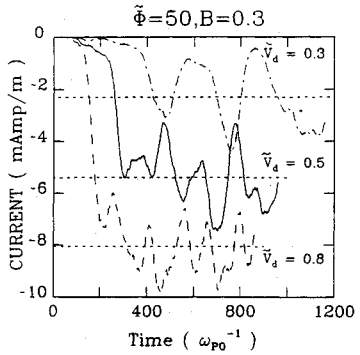

Fig. 3 Temporal evolutions of the currents collected by the cylinder for three flow velocities.

with the drift velocity. A parametric study needed for predicting the current-voltage characteristic of the cylinder has not been completed. However, the limited number of computer runs carried out so far demonstrate that the cross-field plasma transport considerably enhances the collection of electrons.

Figure 3 shows that the oscillations in the current for the low drift velocity $\tilde{V}_0 = 0.3$ are the strongest and also the slowest. As the drift velocity increases, both the oscillation amplitude and the period of the oscillation tend to decrease. Simulations with the real mass of H^+ ions show a similar stabilizing effect of the potential structure. A careful scrutiny of the current oscillations for $\tilde{V} = 0.3$ brings out the processes involved in the enhancement of the current. For this drift, the minimum current $I_{\min} \simeq 0.4$ mA/m and the maximum current $I_{\max} = 5$ mA/m (Fig. 3). The minimum current is found to be roughly given by the geometrical interception of the electrons flowing with the velocity V_0 by the cylinder, i.e.,

$$I_{\min} \sim I = \pi r_s N_0 e V_0 \simeq 0.3 \text{ mA/m} \tag{9}$$

This implies that, during the periods of current minima for $\tilde{V}_0 = 0.3$, the plasma conditions around the cylinders are such that the electrons collected directly come from the unperturbed flow. On the other hand, during the periods of current maxima (Fig. 3), the flow pattern is significantly perturbed, and the topology of the perturbations is such that it leads to a significant enhancement in the collected current. The plasma processes associated with the enhancements are described next.

Cross-Field Plasma Transport

We find that the potential structure around the cylinder plays a key role in the enhancement of the current. If one assumes an azimuthally symmetric sheath with only radial electric fields, the $E_1 \times B_0$ drift is in the azimuthal direction and it completely diverts the electron flow away from the cylinder, causing a complete magnetic insulation of the cylinder from the plasma. In such a case, the electrons circulate around the cylinder and they are not collected by it. Our simulations show that the potential structure near the cylinder is azimuthally asymmetric and the flow pattern around the cylinder is significantly altered.

The temporal evolutions of the current for $V_0 = 0.3$ and of the associated potential structures are shown in Figs. 4. Figures 4b–4f show the potential structures at points b–f marked on the current curve in Fig. 4a. The potential structures are shown by plotting the equipotential surfaces at potential intervals of $\Delta\tilde{\phi} = 5$. We note that the cylinder bias potential $\tilde{\phi}_0 = 50$. For the low drift velocity $\tilde{V}_0 = 0.3$, the equipotentials approximately give the circulation pattern for the electrons, especially in the regions where the equipotentials are closely spaced, giving large electric fields. The sense of the circulation is indicated by the arrows on the equipotentials. Since the ion cyclotron period is very large compared to the ion transit time with velocity V_0 across the simulation system, the ions do not circulate along the equipotentials.

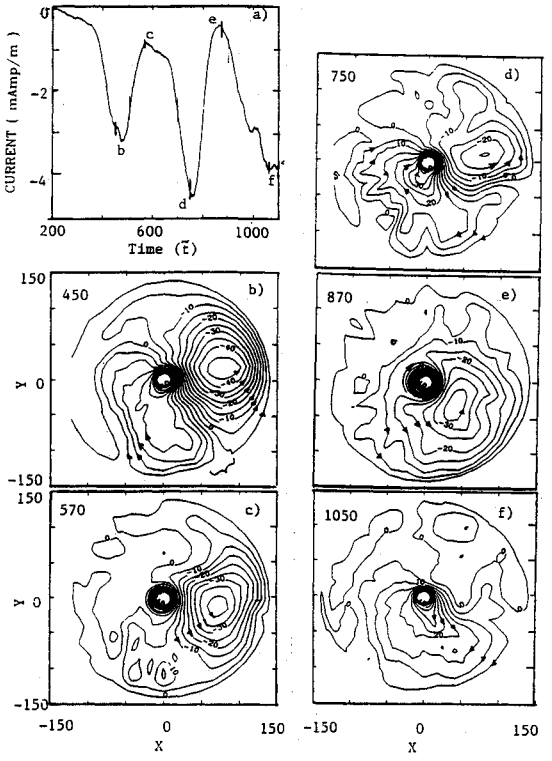

Fig. 4 Temporal evolution of the current for a) $\tilde{V}_0 = 0.3$. Note the points b, c, d, e, and f on the curve. Parts b) through f) show the potential structures around the cylinder at the times corresponding to the above points. The arrows on the equipotential surfaces in parts b) through f) show the circulation of electrons. Note the presence of the fan-shaped circulation pattern at the times of current maxima. The contours are $|\Delta\tilde{\phi}| = 5$ apart.

The potential structure in Fig. 4b shows a two-cell circulation pattern. In the wake region behind a cylinder, the potential is generally negative. For this reason, we call the circulation cell in the wake a negative cell. On the other hand, in the angular region $\pi \lesssim \theta \lesssim 3\pi/2$, the potential is generally positive and the equipotential surfaces are fan shaped. This circulation cell is called a positive cell. The directions of circulations of electrons in the two cells are indicated by the arrows in Fig. 4b. The negative potentials in the wake region are an expected feature because ions are not able to populate this region as effectively as the much more mobile electrons. The formation of the fan-shaped potential structure (Fig. 4b) in the angular region $\pi \lesssim \phi \sim 3\pi/2$ is being reported here for the first time. The main cause of the formation of the fan structure is that in the region near $\theta \sim 3\pi/2$ the azimuthal electron drift in the radial electric fields due to the positive potential on the cylinder is in a direction opposite to the flow velocity V_0. In other words, the radial electric field (E_1) in this region opposes the convection electric field. This leads to the stagnation of plasma near $\theta \simeq 3\pi/2$. This manifests itself in the formation of the fan-shaped structure. The space charges associated with the electron motion in this region create intense azimuthal electric fields in the angular region, indicated by the curly bracket in Fig. 4b. The azimuthal fields are positive (anticlockwise) in this region. The potential drop associated with the azimuthal electric fields and the boundary condition that far from the cylinder $\theta \to 0$ give rise to the fan-shaped potential structure.

The electric fields associated with the fan-shaped potential structure capture the incoming electrons from large distances from the cylinder and circulate them in the close vicinity of the cylinder. This facilitates the collection of a large number of electrons by the cylinder. It is important to note that the potential structures shown in Fig. 4b are not steady; they are obtained by averaging the fields over a time interval $\Delta\tilde{t} = 60$.

If there are fast oscillations in the potential, the electrons can be mixed by moving across the equipotential surfaces. Figure 5 shows a typical example of the oscillations in the potential $\phi(\tilde{r} = 30, \theta = \pi, t)$. There are both slow and fast oscillations. The slow oscillations correspond to the slow oscillation in the current, as shown in Fig. 4a. The fast oscillations are seen to have a period of about $\Delta\tilde{t} = 6$, which is close to the electron-plasma period. These oscillations are relatively weak with amplitudes $\phi_a \lesssim 2kT_0/e$. Since such oscillations perturb the equipotential surfaces at the electron time scale, they are likely to randomize the electron motion over the quasilaminar circulation predicted by the averaged equipotential surfaces shown in Figs. 4. This causes a mixing of electrons across the equipotential surfaces. Thus, the fan-shaped structure provides a large capture area for the collection of electrons by the cylinder.

The two cells in the circulation pattern interact mutually and cause oscillations in both the potential structure and the current. Figure 4c shows that the fan-shaped positive cell has nearly disappeared at $\tilde{t} = 570$ and the negative-potential cell dominates at this time. The cylinder is seen to have a thin sheath in the region $\pi/2 \lesssim \theta \lesssim 3\pi/2$. The sheath thickness is about $\Delta r \sim 10\lambda_d$ in the ram direction ($\theta = \pi$). In this case, the effective electron collecting area of the cylinder is nearly doubled and the expected current $I \simeq \pi(r_s + 10\lambda_{d0})N_0eV_0 \simeq 0.8$ mA/m, which is close to the current as $\tilde{t} = 570$ in Fig. 4a.

Figure 4d shows that the two-cell circulation pattern has reappeared again at $\tilde{t} = 750$ and the current has increased to a maximum of 5 mA/m (Fig. 4a). Since $I_{max}/I_{min} \simeq 12$, the fan-shaped potential structure increases the capture area by this factor. Figures 4e and 4f show that the two-cell pattern disappears at $\tilde{t} = 870$ and reappears again at $\tilde{t} = 1050$, and, correspondingly, the current reaches a minimum followed by a maximum (Fig. 4a). Simulations for H^+ plasma with mass ratio $m_i/m_e = 1836$ show that the amplitudes of the oscillations are considerably diminished giving an approximately constant current.

This discussion clearly demonstrates that the oscillations in the current are controlled by the oscillations in the potential structure around the cylinder. Besides this correspondence in the oscillations in the curent and the potential structure, this discussion also brings out the mechanism of the enhancement in the current collection; the fan-shaped potential structure provides a relatively large capture area for the collection of electrons by the cylinder.

Effect of Flow Velocity on the Current Collection

Figure 3 shows that as the drift velocity increases the periods of oscillation in the current reduce and the currents in the minima increase. Figure 6 shows the temporal evolution of the potential structure for $\tilde{V}_0 = 0.5$ and $\tilde{\phi}_0 = 50$. The important feature of this figure is that the two-cell circulation structure persists continuously, even though it undergoes oscillations. When the positive circulation cell occupies a large area, the collected current is large, and when its area is reduced, so is the collected current. In contrast, for the low drift velocity $\tilde{V}_0 = 0.3$, the fan-shaped positive cell and the negative cell at times disappeared completely, causing relatively large amplitude oscillations in the current.

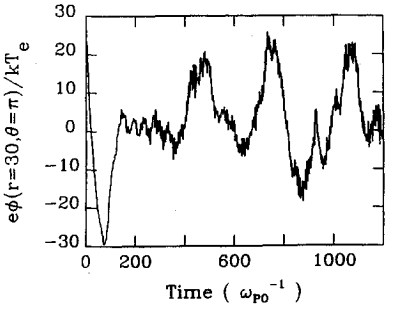

Fig. 5 Temporal evolution of the potential $\tilde{\phi}(\tilde{r} = 30, \theta = \pi, t)$.

We found that the time period of oscillation varies almost inversely with the flow velocity V_0. This suggests the possibility that somehow the oscillation period is related to the transit time of the electrons and ions with this velocity. The electrons are highly magnetized and their cyclotron period is about $\tau_{ce} \approx 20\omega_{p0}^{-1}$, which is much smaller than the oscillation time period $\tau \simeq 250$ for $V_0 = 0.3$. On the other hand, the ion-cyclotron period $\tau_{ci} \simeq 2 \times 10^3\ \omega_{p0}^{-1}$ and the ions are almost unmagnetized for the time scale of the oscillations shown here.

The oscillations between the two cells (Figs. 4) appear to be related to the transit time of ions across the sharp potential drop associated with the azimuthal fields near $\theta \sim 3\pi/2$. This potential drop is like a double layer. The negative potential region in the cell in the wake acts like a cathode, whereas the positive potential region of the fan-shaped cell is an anode. The ion transit time from the anode to the cathode determines the time period of the potential relaxation instability of double layers. Such an instability has been studied in connection with the plasma diodes[7] and it has been studied recently in numerical simulations of double layers.[8] Silevitch[9] has suggested that such an instability may be the cause of flickering auroral brightness.

When ions are accelerated into the negative cell, they neutralize the negative space charge there and raise the plasma potential, and then the positive cell expands toward the wake region, allowing the development of the radially outward electric fields at distances relatively far from the cylinder. This enhances the clockwise azimuthal drift of the electrons. This causes the positive cell to shrink and the negative cell to expand in a clockwise direction. These competitive back and forth motions of the two cells lead to a relaxation type of oscillation in the current (Figs. 3 and 4a) and the potential structure (Figs. 4–6).

Current Strength

The dotted horizontal lines in Fig. 3 show the time-averaged curents for the three normalized drift velocities $\tilde{V}_0 = 0.3$, 0.5, and 0.8, which yield flow velocities ($V_0 = \tilde{V}_0 V_{te}$) 58, 96, and 154 km/s, respectively, for the typical value of $V_{te} = 192.3$ km/s with $T_e = 0.2$ eV. Such flow velocities are quite large for the low Earth orbit. However, the average currents are seen to vary almost linearly with V_0. This allows us to predict the current for other values of the flow velocity. Our simulations reported here are for $\tilde{\phi}_0 = 50$, which gives a bias voltage $\phi_0 = 10$ V with $T_e = 0.2$ eV. For this bias, the current-velocity relation is

$$I \simeq 10\ V_0/V_{te}\ \text{mA/m} \tag{10}$$

For the typical value $V_0 = 8$ km/s of the orbital velocity in the ionosphere, $V_0/V_{te} = 0.04$ and the expected currents $I \simeq 0.4$ mA/m. This magnitude of the current is seen to somewhat increase when simulations are carried out for the H^+ plasma.

It is interesting to compare the previous estimate of the current with that obtained from the theory of Parker and Murphy,[1] which is commonly employed for the calculation of currents in magnetized plasmas of the low Earth orbit. The basic idea behind this theory is as follows. When the electron Larmor radius $\rho_e << a$, the size of the current collecting body transverse to the magnetic field, the electron collection is severely limited, as shown in Fig. 7. Primarily, the electrons moving along the field lines are collected by the body. Parker and Murphy[1] advanced that the $E \times B$ drift in a nonuniform electric field enhances the collection area from body radius a to r_0, where r_0 is given by

$$r_0 \simeq \left\{1 + \left(\frac{8e\phi_0}{m_e\Omega_e^2 a^2}\right)^{1/2}\right\}^{1/2} a \tag{11}$$

where $\Omega_e = eB/m_e$, B being the magnetic field and a the radius

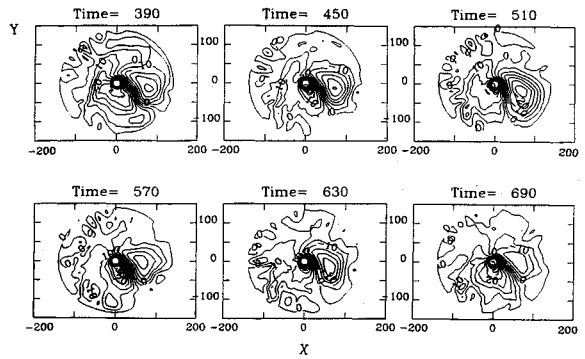

Fig. 6 Temporal evolution of the equipotential surfaces around the cylinder for $\tilde{V}_0 = 0.5$.

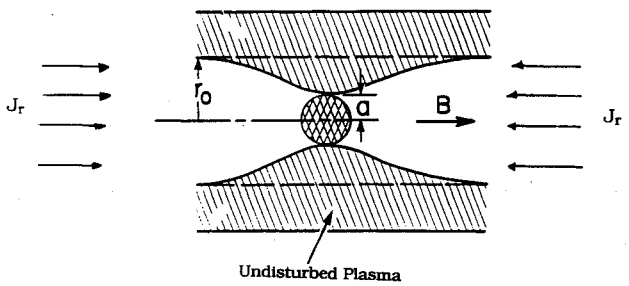

Fig. 7 Current limitation due to the magnetic field; electrons collected by the positive body of radius a are confined within the cylinder of radius r_0 (Ref. 1).

of the body. Although Eq. (11) is derived for a sphere, it is valid when the cylinder is aligned with the magnetic field and the current collection by its ends are considered. In such a case, the projected areas of the sphere and the cylinder on a plane perpendicular to the magnetic field are the same when $a = r_s$. The current collection by the two ends of the cylinder is

$$I_{PM} \leq 2 \times \pi r_0^2 J_r \tag{12}$$

where J_r is the electron thermal current in the plasma and it is given by $J_r = n_0 e V_{te}/\sqrt{2\pi}$ A/m^2, and the subscript PM refers to the current from the Parker-Murphy model.

For the plasma parameters used in the paper and $\phi_0 = 50kT_0/e = 10$ V, $r_0 = 2.86a \simeq 2.86r_s \simeq 0.286$ m, $J_r \simeq 1.22$ mA/m^2, and $I_{PM} \leq 0.62$ mA.

In view of Eq. (10), as noted previously, the current collection entirely due to the cross-field plasma transport is about 0.4 m/Am. This suggests that when an orbiting body of 10-cm radius and about 1 m long is biased 10 V positive with respect to the ionospheric plasma, the cross-field current becomes comparable to that predicted by the Parker-Murphy model. Note that the former current is an additional current, suggesting a current enhancement by a factor of about 2. Simulations with real ion mass for H^+ show that the current enhancements can be even more.

In view of the current-velocity relation in Eq. (10), the excellent comparison between the measured currents collected by a rocket body in the ionosphere[3] and those predicted from the Parker and Murphy model is not surprising. The typical value of the component of the rocket velocity perpendicular to the magnetic field $V_0 \lesssim 100$ m/s, which predicts a negligibly small current ($I \simeq 5$ μ A/m at $\phi_0 = 10$ V) compared to the current (0.62 mA/m) calculated from the Parker-Murphy model.

IV. Conclusions and Discussion

The main conclusions of this paper are as follows.

1) Simulations show that the potential structure around a positively biased cylinder in a plasma flowing perpendicular to the magnetic field is highly asymmetric.

2) The equipotential surfaces indicate the formation of a two-cell circulation pattern for the electrons. Behind the cylinder, where the potential can be negative, the circulation pattern does not include the cylinder. Thus, the electrons in this pattern do not contribute to the current. The fan-shaped circulation pattern with positive potentials, forming in front of the cylinder, includes the cylinder. The electrons circulating in this pattern come in close vicinity of the cylinder.

3) When the fan-shaped pattern is extended over a large area, the collected current is large. On the other hand, when this pattern shrinks to a thin sheath near the cylinder, the current is reduced to the minimum expected value determined by the interception of the electrons flowing with velocity V_0. New simulations with H^+ ions and with a Mach number as low as 4.3, with respect to the ion-acoustic speed, show the formation of the fan-shaped potential structure.

4) The cross-field plasma transport primarily due to the circulation of electrons in the extended fan-shaped potential structure enhances the collected current.

5) The time-averaged enhanced current is found to vary approximately linearly with the relative flow velocity perpendicular to the magnetic field B_0. New simulations with H^+ ions show an even greater enhancement in the current.

6) The current enhancement with the relative flow velocity determined by the orbital velocity (~ 8 km/s) in the low Earth orbit is found to be a significant fraction of the current determined by the Parker-Murphy model, which does not include the cross-field transport of electrons associated with the potential structures in a flowing plasma.

During the preparation of this paper, we have carried out several simulations by varying the relative orientation between the magnetic field and the flow velocity with a real mass ratio for H^+ plasma. The flow velocity has been reduced to as small as $V_0 = 0.1 V_{te}$, which yields a Mach number of 4.3 with respect to the ion-acoustic speed. The basic mechanism for the current enhancement through the cross-field transport of electrons inside the highly asymmetric sheath structure remains generally valid for the relative orientations of V_0, B, and the axis of the cylinder considered in this paper. However, it is found that for H^+ plasma (mass ratio $m_i/m_e = 1836$) the oscillations in the potential structure are not so prominent as seen in the simulation with the artificial mass ratio $m_i/m_e = 100$. But the oscillations seen with the artificial ion mass served the important purpose of demonstrating that the size of the fan-shaped sheath structure plays a key role in the process of current collection. A detailed account of the results from recent simulations covering very low flow velocities and different relative orientations between the flow velocity and the magnetic field will be published elsewhere.[10] However, we point out here that the simulations with $V_0 = 0.1$ for H^+ plasma yield qualitatively similar potential structures, as presented here. A considerable current enhancement is found even with this low flow velocity, which corresponds to a Mach number of 4.3 with respect to the ion-sound speed. In the low Earth orbit, where O^+ ions dominate and the orbital velocity is 8 km/s, the expected Mach number >8. The simulation with the artificial ions presented here cover the Mach number range 3–8. Thus, so far as ion dynamics is concerned, it is well covered by the simulations. The simulation with $\tilde{V}_0 = 0.1$ gives a flow velocity of $V_0 = 192 \times 0.1 = 19.2$ km/s, which is about twice the expected relative flow velocity in the low Earth orbit, and it is not too far from reality. A simulation with even lower flow velocity demands excessively large computer resources and it has not been carried out so far.

In summary, we have reported here the enhancement in the current collection by a positive cylinder in a flowing magnetoplasma through the transport of plasma across a magnetic field. The current enhancement occurs through the modification in the potential structure because of interaction between the flowing plasma and the cylinder.

Acknowledgments

This work was supported by NASA Grant NAGW-1562. The simulation code was developed under a grant from CRAY Research, Inc.

References

[1]Parker, L. W., and Murphy, B. L., "Potential Buildup of an Electron-Emitting Ionospheric Satellite," *Journal of Geophysical Research,* Vol. 72, No. A3, March 1967, pp. 1631–1636.

[2]Linson, L. M., "Current-Voltage Characteristics of an Electron-Emitting Satellite in the Ionosphere," *Journal of Geophysical Research,* Vol. 74, No. A5, May 1969, pp. 2368–2375.

[3]Myers, M. B., Raitt, W. J., Gilchrist, B. E., Banks, P. M., Neubert, T., Williamson, P. R., and Susaki, S., "A Comparison of Current-Voltage Relationships of Collectors in the Earth's Ionosphere with and without Electron Beam Emission," *Geophysical Research Letters,* Vol. 16, No. 5, May 1989, pp. 365–368.

[4]Morse, R. L., "Multidimensional Plasma Simulations by Particle-In-Cell Methods," *Methods in Computational Physics,* Vol. 9, edited by B. Alder, S. Fernbach, and M. Rotinberg, Academic, New York, 1970, pp. 213–239.

[5]Thiemann, H., Singh, N., Schunk, R. W., and Grard, R., "Numerical Simulation of Spacecraft Charging by Impact-Induced Plasmas During a Cometary Flyby," *Journal of Geophysical Research,* Vol. 91, No. A3, March 1986, pp. 2989–3000.

[6]Aldrich, C. H., "Particle Code Simulations Using Injected Particles," *Space Plasma Simulations,* edited by M. Ashour-Abdalla and D. A. Dalton, D. Riedel, Boston, MA, 1985, pp. 131–143.

[7]Burger, P., "Theory of Large Amplitude Oscillations in One-Dimensional Cesium Thermionic Converter," *Journal of Applied Physics,* Vol. 36, No. 6, June 1965, pp. 1938–1943.

[8]Singh, N., and Schunk, R. W., "Current Carrying Properties of Double Layers and Low Frequency Auroral Fluctuations," *Geophysical Research Letters,* Vol. 9, No. 4, April 1982, pp. 446–449.

[9]Silevitch, M. B., "On a Theory of Temporal Fluctuations in the Electrostatic Potential Structures Associated with Auroral Arcs," *Journal of Geophysical Research,* Vol. 86, No. A5, May 1981, pp. 3573–3582.

[10]Singh, N., and Vashi, B. I., "Current Collection Through the Transport of Electrons Across Magnetic Field Lines," Committee on Space Research, Paper MD 3.2.3, July 1990.